TECHNICAL UNIVERSITY OF CLUJ-NAPOCA

ACTA TECHNICA NAPOCENSIS

Series: Applied Mathematics, Mechanics, and Engineering
Vol. 69, Issue I, March, 2026

DESIGN OPTIMISATION OF A CENTRIFUGAL PUMP INDUCER

Viorel BOSTAN, Andrei PETCO, Nadejda PROCA, Dmitrii CROITOR

Abstract: *This article outlines the methodology for developing the geometry of a centrifugal pump inducer through the application of Computational Fluid Dynamics with optimization methods. Numerical simulation of the fluid flow in a centrifugal pump was carried out. Different optimisation algorithms based on the response surface were compared with the best design point. A digital validation of the obtained geometry model was conducted. Cavitation tests of the pump with the original design and with the inducer were performed. The usage of the resulting inducer led to a decrease in Net Positive Suction Head by 0.5 mH2O at the Best Effective Point, which is in accordance with the acquired technical requirements. The obtained inducer was utilized to a produced serial centrifugal canned motor pump by CRIS Hermetic Pumps.*

Keywords: *Inducer, Centrifugal pumps, Computational Fluid Dynamics, Numerical analysis and optimisation methods.*

1. INTRODUCTION

The problem of minimising the Net Positive Suction Head (NPSH) necessary for centrifugal pumps is a fundamental challenge because of their frequent use in low pressure hydraulic systems. One effective method of reducing the required NPSH of a pump is the installation of an inducer, which is an axial flow impeller located upstream of the pump's centrifugal impeller [1]. This research describes an optimisation procedure for an inducer designed for use with a CMP series single-stage hermetic pump produced by CRIS Hermetic Pumps.

Cavitation as a complex physical phenomenon includes a phase transition with heat and mass transfer [2] and can be thought of as a loss of fluid continuity in an area of a reduced pressure [3]. In the event that the inducer is absent, in a centrifugal pump, caverns occur when the fluid pressure at the impeller inlet drops below the saturation pressure of liquid vapours, causing the liquid „boiling up". When the bubbles travel to the high-pressure area downstream of the pump impeller, they collapse, causing a number of negative effects and, if system pressure is below Net Positive Suction Head required (NPSHr), significantly affects pump performance. The cavitation process in centrifugal pumps may arise from multiple factors: unsteady flow with high Reynolds numbers ($Re > 10^5$) [4], complex surface geometry typical of turbomachines and the existence of surface roughness may all lead to the growth of localised cavitation regions [1].

The occurrence of cavitation leads to numerous negative effects on pump operation [1-3]: a mechanical wear of pump components, including erosion, corrosion and cavitation pitting on the surfaces of blades and other wetted components [4] and increases the operating noise and vibrations caused by collapsing vapour bubbles. Contemporary computational software employs models derived from the Rayleigh-Plesset equation [1, 2, 5], which defines the dynamics of spherical vapor bubbles.

2. OPTIMISATION PROCESS DESCRIPTION

2.1 Optimisation task formulation

The selection of appropriate optimisation criteria, parameters and constraints is crucial [6-9]. In this research, the NPSH for a 3% head drops ($NPSH_3$), according to the test procedure

Received: 26.01.26; **Similarities**: 12.02.26: **Reviewed**:26.01. /26.01.26: **Accepted** 17.03.26.

described in ISO 9906:2015 (Hydraulic performance acceptance tests), should ideally have been chosen as the optimisation criterion.

Given the iterative nature of the optimisation, the demands on computational resources and the fact that this requirement is much harder to formalise, a simplified computational model was adopted to reduce the resources required. Instead of modelling the entire fluid domain (Fig.1) including suction and discharge casing sections, impeller and inducer, the computational domain was reduced by a factor of 6.6, covering only the flow region of the inducer.

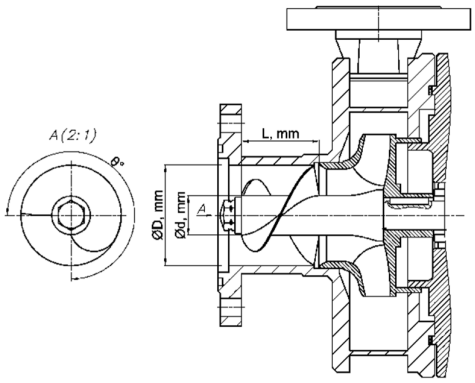

Fig. 1. Drawing of the pump part of a centrifugal pump, indicating the optimisation parameters.

Consequently, the optimisation objective has been altered from directly minimising the NPSHr to maximising the hydraulic head of the inducer, as detailed in 3rd section. The dimensions of the pump inducer were the optimisation parameters.

2.2 Geometric model creation and discretization

The geometric model was created using ANSYS DesignModeler and BladeEditor instrument. The model comprises the fluid region enclosed between the inducer blades, hub, and shroud. A two-blade design was selected (Fig. 2), and the number of blades was not varied during optimization. Due to the axial symmetry of the inducer, only half of the computational zone was required in this simulation.

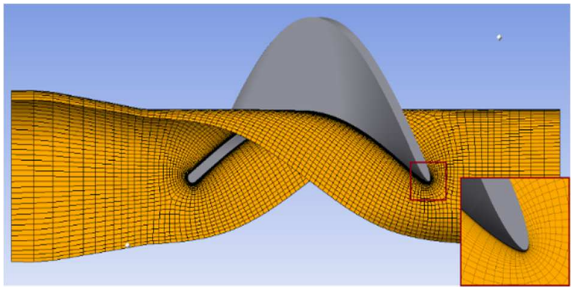

Fig 2. Structured mesh obtained in ANSYS TurboGrid.

The finite volume mesh was generated using ANSYS TurboGrid (Fig. 2), an effective tool for accurately modelling turbomachinery geometries and flow behaviour [6]. Grid generation parameters were set to achieve a target near-wall parameter y^+ of approximately 1, suitable for a Reynolds number of $5 \cdot 10^5$. Structured hexahedral meshes containing 1.5 to 2 million cells were obtained, with a first boundary layer thickness of $5 \cdot 10^{-6}$ m.

2.3 Computational Setup

The boundary and initial conditions employed for the numerical analysis are shown in Fig. 3. The Inlet boundary condition was modelled by liquid water and a total inlet pressure Pinlet of 10^6 Pa. The Outlet boundary condition was established with a constant mass flow rate Qout = 27.78 (kg/s)/z. In this equation, z = 2 represents the inducer blades number.

The impeller domain rotation speed was set at 2950 min^{-1} and the reference pressure Pref is 0 Pa. For the wall surfaces, no-slip conditions were applied, without taking into account the roughness of the inducer flow path surface and gravitational forces. An isothermal flow at a constant temperature of 25°C was assumed for the simulations. Initially, the fluid was considered to be completely liquid water. Due to symmetry, periodic boundary conditions of rotation were applied at the boundaries of the domain.

The physical time scale method was chosen to describe the Timescale. Following the recommendations in [6], various values of the time scale were evaluated, and the value $1/\omega$ = 0.005 s was determined to be optimal, where $\omega = 2\pi n$ denotes the angular velocity. For interdomain interactions, the Frozen Rotor interface model was chosen, which provides high accuracy in simulating fluid flow while

capturing detailed interactions between domains [6].

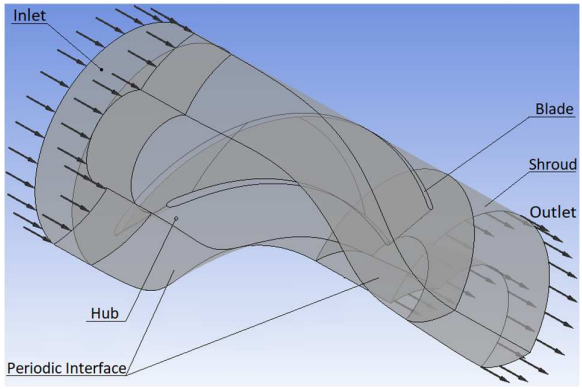

Fig. 3. Application of boundary and initial conditions.

A *RANS (Reynolds-averaged Navier-Stokes)* steady-state method, with turbulence simulation using *k-omega SST model* [10], was used. The SST model is one of the main models applied to turbulence modelling [11-13]. Cavitation modelling was performed using the Rayleigh–Plesset equation-based Zwart, Gerber, and Belamri model [13, 14].

2.4 Processing, post-processing and data selection

Fig. 4 illustrates the dimensionless wall-distance parameter y^+ distribution across inducer blades and hub surfaces, confirming suitability for accurate boundary-layer grid resolution. The observed values remained stable within the range of units, indicating good grid quality [11].

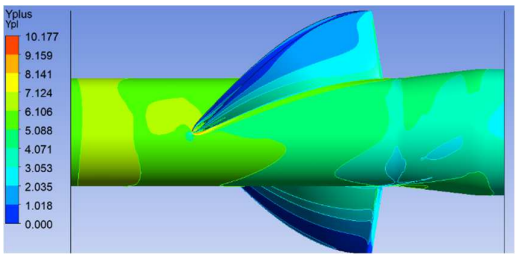

Fig. 4. y+ parameter distribution on the hub and blades surfaces.

Simulations were iteratively executed in ANSYS Workbench, terminating after reaching either a maximum iteration limit of 250 or a residual tolerance of 10^{-5}. Static pressures at domain inlet and outlet, torque on the inducer's rotational axis, and mass flow imbalances served as convergence criteria.

3. OPTIMISATION PROCESS

3.1 Setting parameters and optimisation criteria

The optimisation process was carried out using ANSYS optiSLang software. The maximum achievable pressure generated by the inducer was selected as the main optimisation criterion. The advantage of this criterion is a significant reduction in computing resources, but its limitation is that it ignores the reciprocal hydraulic interaction between the pump impeller and the pump inducer, since the inducer is analysed independently of the rest of the pump flow.

The geometrical model of the inducer was parameterised using four key geometric parameters: inducer length (*L*), hub diameter (*d*), diameter of the inducer (*D*) and blade wrap angle (θ), as shown in Fig. 1. The permissible ranges of parameter variation presented in Table 1 were limited by the existing design specifications of the manufactured pump, which significantly restricted the possible variations in the diameter of the inducer (*D*) and its length (*L*).

Table 1.

Optimisation parameters limits.

Hub diameter d, mm	Wrapping angle θ, °	Diameter of the inducer (D, mm	Length L, mm
36 ÷ 50	-360 ÷ -90	80 ÷ 105	50 ÷ 86

The Latin hypercube sampling (LHS) approach was employed to systematically produce random combinations of parameters within defined constraints, yielding a total of 120 design points. This ensured adequate coverage of the design space.

3.2 Data analysis and processing

Following parameter sampling, CFD simulations were performed to evaluate inducer performance at the selected design points. The resulting simulation dataset was imported into ANSYS optiSLang for further statistical analysis. Out of the 120 generated design points, 98 valid simulation outcomes were evaluated. A linear regression method was employed on the acquired dataset to construct a response surface, as illustrated in Fig. 5.

The response surface analysis (Fig. 5 (b)) revealed that inducer geometries with wrapping angles (θ) below approximately 200-250 degrees

generally exhibit negative head development, as indicated by outlet pressures consistently lower than inlet pressures. This phenomenon occurs due to excessively narrow flow cross-sectional areas.

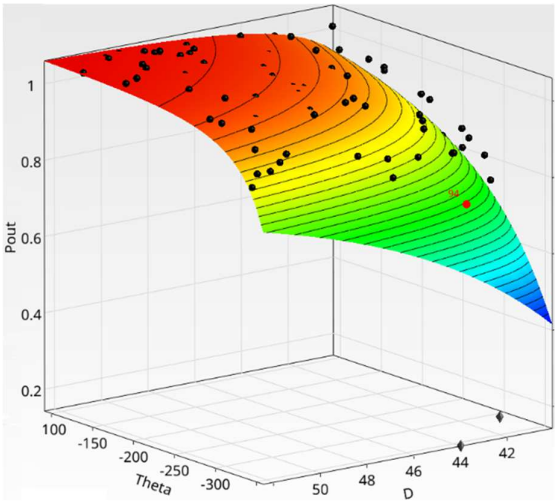

(a)

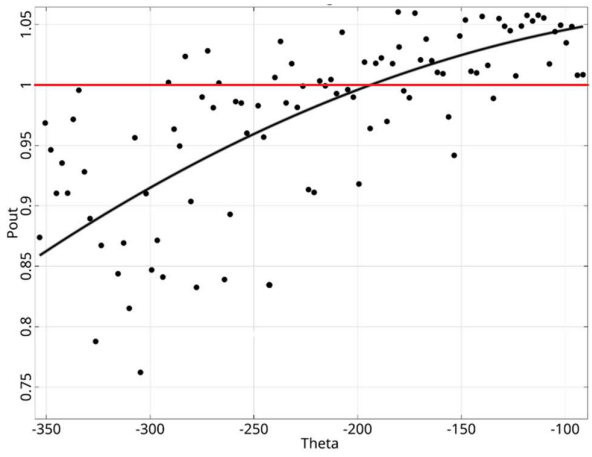

(b)

Fig.5. Response surface representation: (a) wrapping angle θ and the outer diameter D vs. developed head; (b) wrapping angle θ vs. developed head.

The correlation matrix of the geometric parameters of the inducer (Table 2) and their influence on the performance of the inducer head was analysed to identify the strength and nature of the relationships between the various geometric characteristics.

Table 2.

Correlation matrix.

	θ	D	L	d	H
θ (Wrapping angle)	1.00	-0.06	-0.05	0.03	0.68
D (Ind. diameter)	-0.06	1.00	-0.02	0.04	0.48
L (Length)	-0.05	-0.02	1.00	0.02	0.32
d (Hub diameter)	0.03	0.04	0.02	1.00	-0.05
H (Inducer Head)	0.68	0.48	0.32	-0.05	1.00

The outer diameter (D) showed a positive correlation (0.48) with the inducer head, indicating that increasing the outer diameter has a positive effect on the performance of the inducer head. In addition, the wrapping angle (θ) showed the strongest positive correlation (0.68) with the performance of the inducer head. Overall, both parameters boil down to the cross-sectional area of the inducer channel as a criterion for fluid flow and its importance in the optimisation process.

As optimisation algorithms, were selected the following: Adaptive Response Surface Method (ARSM), Evolutionary Algorithm (EA) and Non-Linear Programming by Quadratic Lagrangian (NLPQL). The optimization results derived from the aforementioned methods were compared with the most efficient design point. The optimal outcome was demonstrated by the geometry derived from the most efficient design point parameters, where the inducer's head measured approximately H = 51.5 kPa (Tab.3).

Table 3.

Optimisation results.

Optim. method	d, mm	D, mm	L, mm	θ, °	Head H, kPa
EA	46.96	103.5	81.0	-90.0	4.63
ARSM	47.7	104.8	50.0	-91.0	4.29
NLPQ	46.04	104.8	66.0	-92.6	4.25
Best DP	41.12	104.1	77.1	-180.4	5.26

The results were numerically validated (Fig. 6 (a), (b)) through CFD simulations of fluid flow in the complete pump assembly. The value of $NPSH_3$ was determined by progressively decreasing the inlet pressure.

It was observed that achieving computational convergence at pressures close to $NPSH_3$ posed significant challenges due to increased numerical instability and computational domain imbalance. Simulation results at pressure near $NPSH_3$, demonstrated cavitation cavity patterns consistent with experimental observations reported previously in the literature [15–17]. At pressures below the calculated NPSH3 (Fig. 6 (a)), cavitation cavities spread to the front edges of the impeller blades (Fig. 6 (b)), reducing the volume fraction of liquid in the flow.

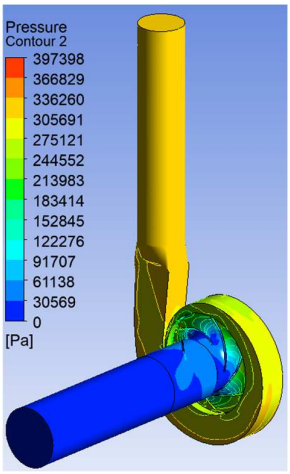

(a)

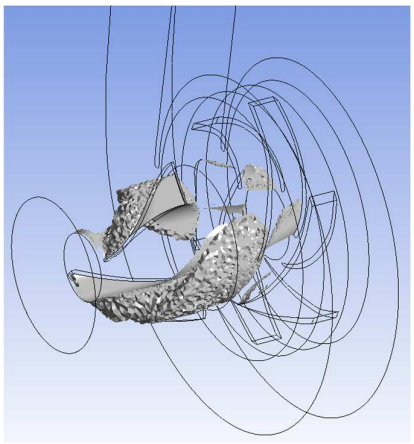

(b)

Fig. 6. Results of digital validation: (a) Distribution of the pressure field; (b) Cavitation caverns representation at NPSH = 2.6 mH2O.

3.3 Experimental verification of optimisation results.

Experimental verification of the inducer optimization was performed using a centrifugal pump from the CMP series, tested according to ISO 9906 : 2015 standards.

The objective of the test (Fig. 7 (a), (b)), besides acquiring the primary characteristics of the pump (developed pump head, current consumption, and power), was to determine the value of NPSH3, the net positive suction head available for the test pump at a constant flow, when the pump head is diminished by 3% due to cavitation resulting from a reduction in available suction head.

The experimental test (Fig. 7 (a), (b)) aimed to evaluate pump head performance, current consumption, power requirements, and specifically to determine the $NPSH_3$ value - the available net positive suction head at constant flow, corresponding to a 3% reduction in total pump head due to cavitation-induced head loss [18].

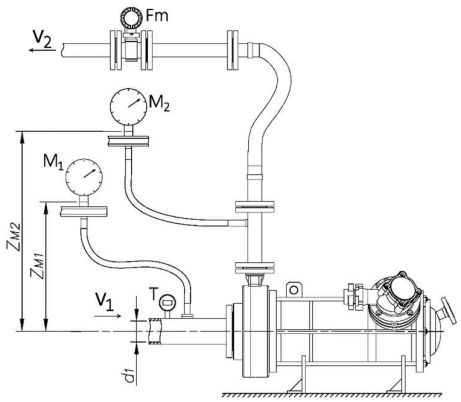

(a)

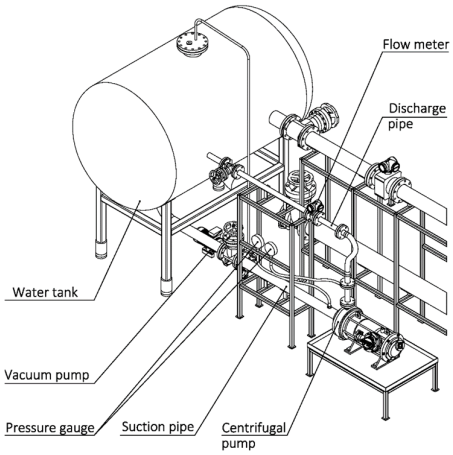

(b)

Fig. 7. Centrifugal pump testing: (a) test scheme, (b) structure of the test station.

During the test (Fig.8 (a)), a closed testing scheme was used, the fluid flow rate was used as a constant and the tank pressure designated as the independent variable. Cavitation tests were carried out with clean cold water, with the temperature monitored by T thermometer for the precise density calculation. The centrifugal pump was turned on, with the set flowrate (measured by Fm flow meter), corresponding to the flow at the desired point, the pressure was measured by M_1 pressure gauge. Measurements were made iteratively, with a certain interval of pressure drop in the tank. In the case of a pressure drop of 3%, the value P_{M1} on the M_1 pressure gauge is registered in order to obtain the $NPSH_3$ value calculated by the formula (1).

$$NPSH_3 = 0.102\frac{\pm P_{M1} + P_b - P_v}{\rho} + Z_{M1} + 0.0827\frac{Q^2}{d_1^4}, (1)$$

where: Q is the value of the flow rate passing through the suction pipe with a diameter d_1, P_b represents barometric pressure, P_{M1} is the pressure value at pressure gauge M_1 and vertical mark of the pressure gauge M_1 position.

(a)

(b)

Fig. 8. Experimental validation of the optimisation process results: (a) Pump testing; (b) Manufactured inducer and impeller.

The NPSH3 value is essential to prevent cavitation and is utilized to determine the optimal NPSHr value:

$$NPSHr = NSPH_3 + P_v + 0.5\,mH2O. \quad (2)$$

The experimentally determined $NPSH_3$ value at the Best Efficiency Point (BEP) was 2.60 mH_2O, corresponds with the technical specifications. The experimental results, illustrated in Fig. 9, reveal an overall $NPSH_3$ reduction of approximately 0.5 mH_2O compared to the original configuration, consistent with theoretical predictions.

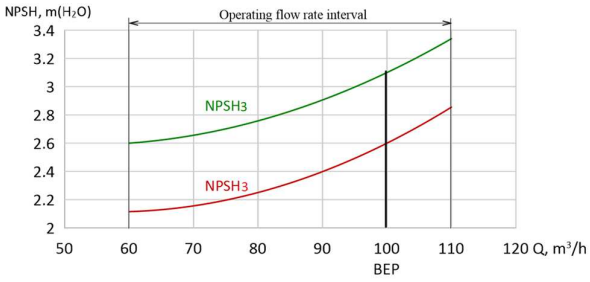

Fig. 9. Cavitation characteristics.

4. CONCLUSION

This research involves the design of a centrifugal pump inducer utilizing CFD methodologies in combination with optimisation techniques. The selected geometric model, while not fully optimal, allows a full-fledged optimisation process with significant savings in computational resources.

As part of the research, various optimisation algorithms were evaluated based on the response surface constructed from 98 design points. The maximum head was achieved by the geometry corresponding to the best-performing design point. Digital validation of the optimisation results was carried out, showing good correlation with experimental data.

A digital verification of the optimization method outcomes was conducted, which correlate with empirical data. Cavitation tests were carried out on the pump with the original design and with the inducer. The usage of the resulting inducer led to NPSH3 reduction by 0.5 mH2O at the Best Efficiency Point, aligning with the technical specifications. The resulted inducer was utilized in a serial centrifugal canned motor pump produced by CRIS Hermetic Pumps.

5. REFERENCES

[1] Gülich, J.F., *Centrifugal Pumps*. Springer International Publishing, ISBN: 978-3-030-14787-7, Cham, 2020.

[2] *A Sustainable Europe by 2030 - European Commission.*

https://commission.europa.eu/publications/sustainable-europe-2030.

[3] Bostan, V., Petco, A., *Minimizing blade-fluid energy energy losses in centrifugal hydraulic pump impellers*, ACTA Tech. Napoc. Appl. Math. Mech. Eng. vol. 67, no. 2S, ISSN 1221 – 5872, Cluj, Romania, Oct. 2024

[4] Petco, A., *Increasing the energy efficiency of centrifugal pumps through mathematical modeling and numerical computation of fluid flow*, Technical University of Moldova, Chisinau, https://anacec.md/files/Petco-teza.pdf, 2024.

[5] Moisă, I. G., Susan-Resiga, R., Muntean, S., *Pump inducer optimization based on cavitation criterion*, Proceedings of the Romanian academy, series A, Volume 14, Number 4/2013, pp. 317–325, The Publishing House Proceedings of The Romanian Academy, 2013.

[6] Parikh, T., Mansour, M., Thévenin, D., *Maximizing the performance of pump inducers using CFD-based multi-objective optimization*, Struct. Multidiscip. Optim. vol. 65, no. 1, p. 9, Dec. 2021.

[7] Zhang, Y., Hu, S., Wu, J., Zhang, Y., Chen, L., *Multi-objective optimization of double suction centrifugal pump using Kriging metamodels*, Adv. Eng. Softw. vol. 74, pp. 16-26, Aug. 2014.

[8] Abdolahnejad, E., Mahdi, M., Shahram, D., *Optimization of Centrifugal Slurry Pump Through the Splitter Blades Position*, 2021.

[9] Kim, B., Siddique, M. H., Samad, A., Hu, G., Lee, D.E., *Optimization of Centrifugal Pump Impeller for Pumping Viscous Fluids Using Direct Design Optimization Technique*. Machines 10 (9) 774, 2022.

[10] Mălăel, I., Gherman, G.B., *Numerical Investigation of a New LH2 Centrifugal Pump Concept Used in Space Propulsion*. INCAS BULLETIN 10 (June), pp. 65–74, ISSN 2247–4528, 2018.

[11] Li, S.C., *Cavitation of Hydraulic Machinery*, vol. 1. in Series on Hydraulic Machinery, Imperial College Press, ISBN 1860942571, London, 2000.

[12] Franc, J.-P., *The Rayleigh-Plesset equation: a simple and powerful tool to understand various aspects of cavitation*, in *Fluid Dynamics of Cavitation and Cavitating Turbopumps Springer*, pp. 1-41, ISBN 978-3-211-76668-2 Cham, 2007.

[13] Franc, J.-P., Michel, J.-M., *Fundamentals of Cavitation*, Springer Netherlands, ISBN 978-1-4020-2232-6, Dordrecht, 2005.

[14] Bostan, V., *Mathematical models in engineering: contact problems: numerical modeling and simulation in aero-hydrodynamics*., S.N., ISBN 978-9975-80-831-6, Chisinau, 2014.

[15] Zwart, P., Gerber, A. G., Belamri, T., *A two-phase flow model for predicting cavitation dynamics*, Fifth Int. Conf. Multiph. Flow, ICMF 2004 International Conference on Multiphase FlowYokohama, Japan, May 30-June 3, 2004.

[16] Xie, S., Wang, Y., Liu, Z., Zhu, Z., Ning, C., Zhao, L., *Optimization of centrifugal pump cavitation performance based on CFD*, International Symposium of Cavitation and Multiphase Flow, ISCM 2014, IOP Conf. Series: Materials Science and Engineering 72, IOP Publishing, 2015

[17] Qiu, N., Wang, L., Kong, F., Wu, D., *Research on cavitation characteristic of inducer*, IOP Conf. Ser. Mater. Sci. Eng, vol. 52, Nov. 2013.

[18] International Organization for Standardization, *ISO 9906:2012 Rotodynamic pumps - Hydraulic performance acceptance tests - Grades 1, 2 and 3,* iso.org/standard/41202.html

[19] Bostan, V., Petco, A., *Determining optimal simulation settings for the centrifugal pump parts optimization process.*, *J. Eng. Sci.* no. 30 (2), pp. 8-22, ISSN 2587-3474, 2023.

[20] Menter, F. R., *Two-equation eddy-viscosity turbulence models for engineering applications*, AIAA J., vol. 32, no. 8, pp. 1598-1605, 1994.

Optimizarea constructivă a impulsorului unei pompe centrifugale

Rezumat: Acest articol prezintă procesul de creare a geometriei impulsorului pompei centrifugale prin aplicarea Dinamicii Fluidelor Computaționale în combinație cu metode de optimizare. A fost prezentată simularea numerică a fluxului de fluid într-o pompă centrifugală. Diferiți algoritmi de optimizare ce se bazează pe RSM au fost comparați cu o geometrie obținută aleatoriu cu cel mai bun rezultat. A fost produsă o verificare digitală a modelelor geometrice obținute în cadrul procesului de optimizare. Au fost realizată testarea în regim de cavitație a pompei conform proiectului inițial și cu impulsor. Aplicarea impulsorului obținut a condus la o micșorare a înălțimii nete pozitive de aspirație NPSHr cu 0,5 mH2O la cel mai bun punct efectiv, ceea ce se conformează cu specificația obținută. Inductorul rezultat a fost aplicat unei pompe de serie produse de CRIS Hermetic Pumps.

Viorel BOSTAN, prof., dr. hab., Technical University of Moldova, viorel.bostan@adm.utm.md, Rep. Moldova, Chisinau, Stefan cel Mare Avenue, 168.

Andrei PETCO, lect. univ., dr., Technical University of Moldova and Design Engineer at S.R.L. "CRIS", andrei.petco@tcm.utm.md, Republic of Moldova, Chisinau, Studentilor str. 9/8, of.220.

Nadejda PROCA, Process Engineer and Head of Quality Control Department, S.R.L. "CRIS", nadejda.proca@crispumps.md, Republic of Moldova, Chisinau, Albisoara St. 68/2, 69.

Dmitrii CROITOR, Master's student, Technical University of Moldova, dmitii.croitor@if.utm.md, Republic of Moldova, Chisinau, Studentilor str. 9/8, of.220.